

## Influences of component ratio of minor phases and charge sequence on the morphology and mechanical properties of PP/PS/PA6 ternary blends

Yan Li · Dong Wang · Jia-Min Zhang · Xu-Ming Xie

Received: 16 May 2010 / Revised: 7 July 2010 / Accepted: 15 September 2010 /

Published online: 8 October 2010

© Springer-Verlag 2010

**Abstract** In this study, influences of both component ratio of minor phases and charge sequence on the morphology and mechanical performance in typical ternary blends, polypropylene (PP)/polystyrene (PS)/polyamide-6 (PA6), have been studied. Reactive compatibilization of the blends has been carried out using multi-monomer melt grafted PP with anhydride groups and styrene segments. For uncompatibilized blends, scanning electron microscope (SEM) and selective solvent extraction showed that the blends presented a core–shell morphology with PS as shell and PA6 as core in the PP matrix, in spite of the component ratio and charge sequence. The shell thickened and droplet size decreased with increasing the PS/PA6 component ratio. While for compatibilized blends, the addition of compatibilizers resulted in a significant reduction of the dispersed droplet size and the phase structure of the dispersed phases was greatly dependent on the charge sequence. When the blending of PA6, g-PP, and PP are preceded, the encapsulation structure reversed into the structure of PS phase encapsulated by PA6 phase, which led to better tensile and flexural strength of the blends.

**Keywords** Morphology · Charge sequence · Component ratio

---

Y. Li · D. Wang · X.-M. Xie (✉)

Advanced Materials Laboratory, Department of Chemical Engineering, Tsinghua University,  
Beijing 100084, China  
e-mail: xxm-dce@mail.tsinghua.edu.cn

J.-M. Zhang

School of Chemistry & Chemical Engineering, Henan Institute of Science and Technology,  
Xinxiang, Henan 453003, China

## Introduction

As is known for polymer blends, the outstanding performance results from not only the blend components but also the multiphase morphologies [1, 2]. Therefore, more and more attention has been paid to the prediction and control of phase morphology of polymer blends [3–9]. So far, in spite of many studies on the morphology of polymer blends, only few of the researchers have focused on the phase morphology of multiple component polymer blends, which is very crucial for new materials creation, plastics recycling, and reusing.

In 1980s, Hobbs et al. [10] applied Harkin's spreading coefficient concept to predict the type of the phase morphology developed in a ternary immiscible polymer blend in which two distinct phases are dispersed in a matrix phase.

Some researchers [1, 11–16] also introduced the predictions of minimum free energy theory and dynamic phenomenological model. Although these theories could predict many of the morphology of multiple component blends, it is difficult to obtain accurate interfacial tension data on static interfacial tensions [17–19]. Moreover, the phase morphologies of multi-component blends have been reported to be controlled not only by the interfacial tensions, the melt viscosity, but also by thermodynamics and kinetic factors [20–22].

Besides, for multiple component polymer blends, the interfacial adhesion of polymer blends is usually very weak, compatibilizers should be added. The addition of compatibilizers would increase the parameters to control the morphology and, however, there is rarely effective compatibilizer for multiple component polymer blends.

Therefore, though some studies are related to morphologies of multiple component blends that contain three or more than three immiscible components, only a few dealt with compatibilized blends [2, 23–32]. Horiuchi et al. [2] studied the morphology development of ternary immiscible blends (PA6/polycarbonate(PC)/SEBS and PA6/PC/PS) through an interfacial reaction between components. Maleinated SEBS (SEBS-g-MA) or maleinated PS (PS-g-MA) was incorporated with its unmodified polymer (un-SEBS and un-PS, respectively) at various ratios into the blends of PA6/PC. The blends of PA6/PC/un-SEBS and PA6/PC/un-PS show a similar phase formation in which the two-dispersed polymers are stuck together in a PA6 matrix. Omonov et al. [24] investigated phase morphology development in PA6, PP, and PS ternary blends, uncompatibilized or compatibilized. They used two reactive compatibilizers: PP-g-MA and SMA for PA6/PP and PA6/PS, respectively. Freitas et al. [27] did research on the evolution of the morphology of PP/PS/PMMA blends with graft copolymers PP-g-PS of two compositions (55/45 and 70/30), PP-g-PMMA or SEBS. In our previous work [32], a multi-monomer melt grafted PP functionalized with maleic anhydride and St (PP-g-(St-*co*-MAH)) was used to investigate the phase morphology of the PP/PA6/PS blends. It was also found that the addition of PP-g-(St-*co*-MAH) leads to smaller and more uniform compatibilized blends than PP-g-MAH, PP-g-St, and their mixture.

In brief, it is very important to understand and control the complicated morphologies for multiple component polymer blends.

In this article, the influences of blending time, component ratio of minor phases, and charge sequence on the morphology of the uncompatibilized PP/PS/PA6 blends

by scanning electron microscope (SEM) are discussed in detail. In addition, the effect of charge sequence on the morphology development is also investigated by adding PP-*g*-(St-*co*-MAH), prepared by multi-monomer melt grafting. The relative role of morphology to mechanical properties of both uncompatibilized and compatibilized blends is also addressed.

## Experimental

### Materials

Both isotactic polypropylene (PP, S1003) and polystyrene (PS, 666D) were obtained from Yanshan Petrochemical Company. The melt flow rate index (MFR) values of the samples are 3.4 g/min and 8.0 g/10 min measured by ASTM D1238 under the condition of 2.16 kg and 230 °C, respectively. Polyamide (PA6, 1013B) was from Ube Company.

The compatibilizer, PP-*g*-(MAH-*co*-St), was multi-monomer melt grafted in our laboratory according to the published literatures [32–34]. The graft degrees of the MAH and St monomers are 0.68 and 0.93 wt% in PP-*g*-(MAH-*co*-St), respectively.

All polymers were dried in an oven at 80 °C for 8 h before use.

### Sample preparation

#### *PP/PS/PA6 blend compositions*

The blends for morphology investigation were prepared in a Haake Rheomix 600 batch mixer. The detailed formulation of the blend compositions is listed in Table 1. Samples 1–3 and 13 were prepared by single processing, while the other samples were prepared with different charge sequence.

#### *Blend sample preparation*

*Blend samples for morphology investigation prepared by Haake mixer* Preparation of the blends for morphology investigation was carried out in the Haake rheomixer. Pellets of the components were dry blended prior to the melt blending. The temperature was set at 240 °C for all three heating sections. The rotation rate of the roller blades was kept constant at 80 rpm.

For the preparation process, a flow chart was shown in Fig. 1. As an example, for sample 4 preparation, the blended PP and PS were first put into the Haake rheomixer to blend for 7 min, then PA6 pellets were added and further blended for another 7 min. After blending for a fixed time, the blended samples were quenched in cold water to fix the morphology.

*Blend samples for mechanical property investigation extruded by twin screw extruder* The samples for mechanical tests were prepared by melt blending using a co-rotation twin-screw extruder with a screw diameter of 35 mm and L/D ratio of

**Table 1** Formulation of the blending compositions

Sample name	Constituent			
	Major phase PP (wt%)	Minor phase PA6 (wt%)	Minor phase PS (wt%)	Compatibilizer PP-g-(MAH- <i>co</i> -St) (wt%)
1	70	7.5	22.5	
2	70	15	15	
3	70	22.5	7.5	
4	70	15	15	
5	70	15	15	
6	70	15	15	
7	70	12.5	12.5	5
8	70	12.5	12.5	5
9	70	12.5	12.5	5
10	70	12.5	12.5	5
11	70	12.5	12.5	5
12	70	12.5	12.5	5
13	70	12.5	12.5	5

48. The screw rate was also set at 80 rpm. The barrel of the extruder has seven temperature-control zones and their temperatures were set at 200–210–220–230–240–240–230 °C (from hopper to die). The pelletized blends were dried at 80 °C for 8 h and then injection molded into standard ASTM specimens with a ZT-630 injection molding machine for mechanical tests.

All the ingredients of the components were fed into the barrel as described in Table 1, and the blend samples were also prepared according to Fig. 1.

## Characterization

### SEM observation

The morphology of the blends was observed with a JSM-7401F (Hitachi) scanning electron microscope (SEM). The blend samples were fractured cryogenically, and to obtain a good contrast between the phases in ternary blends, samples were then stirred in a Formic acid or THF at 50 °C for 8 h to extract the PA6 or PS phase, respectively. Each of the samples was coated with 20-nm thick gold using a sputtering coater. The accelerating voltage was set to 20 kV.

### Mechanical tests

Mechanical property measurements of the samples were carried out according to ASTM standards at room temperature. Tensile and flexural tests were carried out using a GOTECH-2000 universal testing machine. The test speeds were set at 50 mm/min. The average of at least five measurements for each blend was reported.

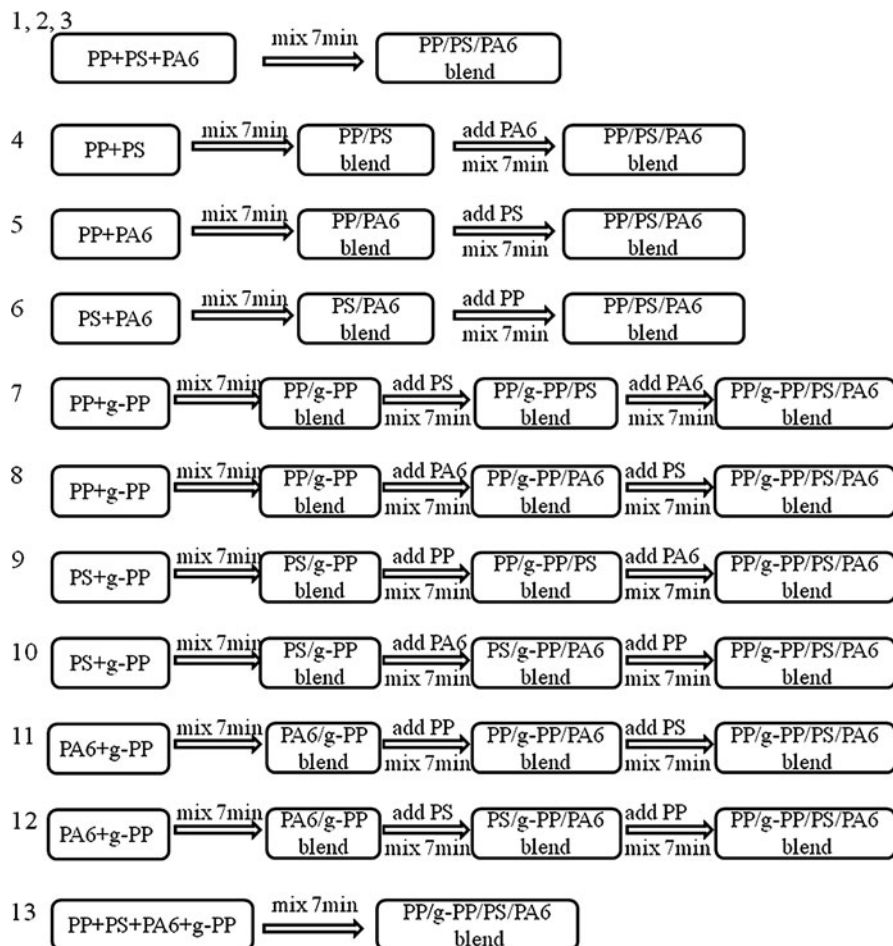


**Fig. 1** The flow chart of the procedure

The Izod notched impact strength of the materials was measured with an XJUD-5.5 impact-testing machine. For each kind of blends, seven specimens were tested and the average value was given.

## Results and discussion

### SEM observation

#### *Effect of blending time on the phase morphology of uncompatibilized PP/PA6/PS (70/15/15 wt%) blends*

Figure 2 shows SEM micrographs of the morphology evolution of the uncompatibilized PP/PS/PA6 blends as a function of blending time. The surfaces were all

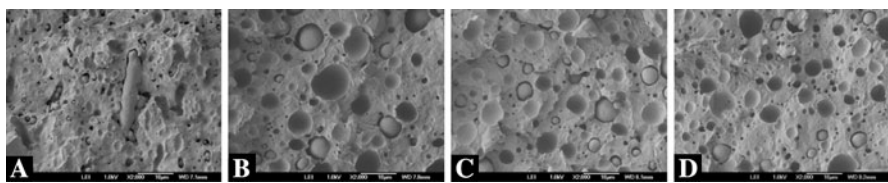


**Fig. 2** SEM micrographs of cryofractured surfaces of PP/PA6/PS (70/15/15 wt%) ternary blends of different blending time just after melt processing. The PS phase has been selectively extracted using THF. **a** 1 min; **b** 5 min; **c** 7 min; **d** 10 min

cryofractured, and the PS dispersed phase was etched by THF. Within the first minutes of blending, the dispersed PA6 and PS phases in PP matrix were first aggregated and elongated (Fig. 2a) and then broke into round droplets with different sizes (Fig. 2b). The size of the dispersed phase was continuously reduced with increasing the blending time as shown in Fig. 2c and d, until the collision and breaking of the dispersed phase which occurred simultaneously reached a balance during the continuous shearing. The dispersed droplets seemed to be stable after about 5 min blending. Through the overview of SEM images, it should be better to choose 7 min blending for the sample preparation. In Fig. 2b and c, there are voids between some PA6 droplets and PP matrix after removing PS phase, implying a core–shell morphology with PA6 droplets inside the PS shell existed in the PP/PS/PA6 blends. Meanwhile, there were also some droplets of PA6 phase and PS phase dispersed in the PP matrix individually.

For the ternary system with PA6 and PS as the dispersed phases and PP as the continuous phase, the type of phase morphology can be predicted by the spreading coefficient, as given by Eq. 1 [10]. If the value of the spreading coefficient  $\lambda_{PS/PA6}$  of the PS phase on the PA6 phase is positive, PA6 phase would be encapsulated by PS phase in PP matrix.

$$\lambda_{PS/PA6} = \sigma_{PP/PA6} - \sigma_{PP/PS} - \sigma_{PS/PA6}, \quad (1)$$

where  $\sigma_{ij}$  is the interfacial tension between  $i$  and  $j$  components.

As calculated from Eq. 1 by the values of literature data [24, 35] of the interfacial tensions among PA6, PP, and PS, the value of  $\lambda_{PS/PA6}$  is indeed positive, implying PS phase would encapsulate PA6 phase during blending. This was consistent with the morphologies shown in Fig. 2.

#### *Effect of component ratio of minor phases on the phase morphology of the PP/PA6/PS blends*

Morphologies of samples 1–3 with the component ratio of PS and PA6 phases ranging from 3:1 to 1:3 in the PP matrix were presented in Fig. 3. As shown, from the void size between PA6 phase and PP matrix, the thickness of the PS shell decreased with decreasing the component ratio of PS and PA6. The less the content of PS phase, the thinner the shell was. In spite of the component ratio of minor phases, the encapsulated morphology was maintained in PP/PS/PA6 blends, suggesting that the morphology type of the ternary blends is unaffected by the

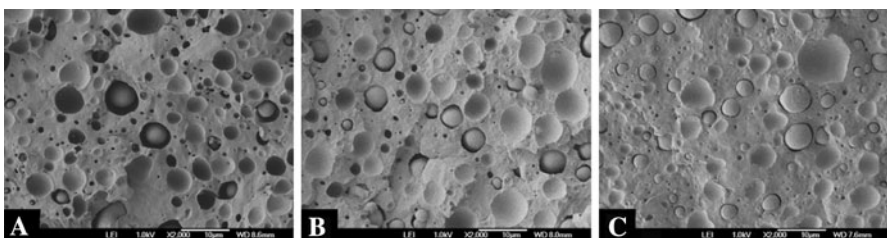


**Fig. 3** SEM micrographs of morphology of PP/PS/PA6 ternary blends of different component ratios. The PS phase has been selectively extracted using THF. **a** 70/22.5/7.5; **b** 70/15/15; **c** 70/7.5/22.5

component ratio of minor phases, and only according to the spreading coefficient method.

#### *Effect of charge sequence on the phase morphology*

For uncompatibilized systems, there are three different charge sequences to prepare the blends. Figure 4 shows the morphology of the uncompatibilized PP/PS/PA6 blends with different charge sequence. The morphologies were not influenced by the charge sequence, and the morphology of PA6 droplets encapsulated by PS phase was maintained due to the weak interaction among the phases for the uncompatibilized PP/PS/PA6 blends.

However, in the presence of compatibilizer, the morphology of the blends would be very complicated because of both chemical and physical interactions among the compatibilizers and phases. Once blended together, the morphology of the blends would be determined by the preferred reaction or interaction between the components. Therefore, charge sequence should play a very important role in compatibilized systems. Thus, six different charge sequences shown in Fig. 1 were designed, and the corresponding samples were prepared as samples 7–12.

Figure 5 shows the SEM images of the compatibilized PP/PS/PA6 blends for samples 7–12 by selectively extracted for PS phase, and Fig. 6 shows the SEM images of the compatibilized PP/PS/PA6 blends for samples 7–12 by selectively extracted for PA6 phase. In Fig. 5, it could be seen that the morphology of PS encapsulated PA6 phase existed in all charge sequences. The addition of compatibilizers resulted in a significant reduction of the dispersed droplet size.

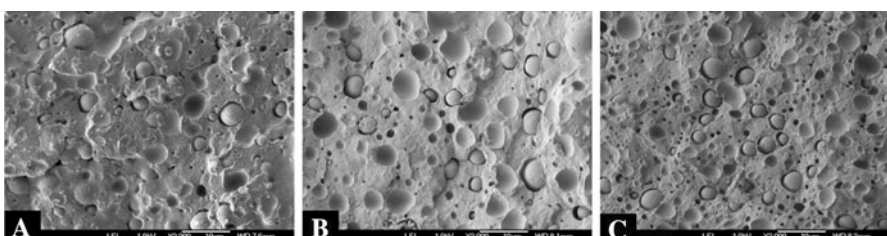


**Fig. 4** SEM micrographs of morphology of PP/PA6/PS (70/15/15 wt%) ternary blends of different charge sequence immediately after melt processing. The PS phase has been selectively extracted using THF. **a** Sample 4; **b** sample 5; **c** sample 6

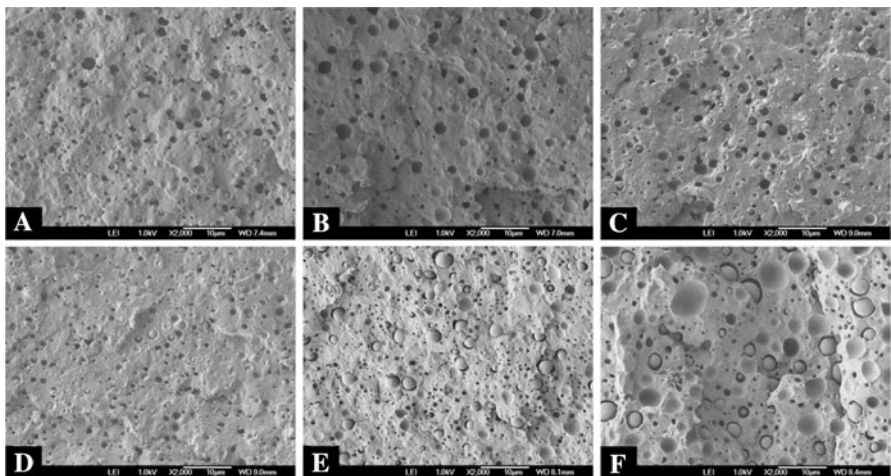


**Fig. 5** SEM micrographs of morphology of PP + PP-g-(MAH-*co*-St)/PA6/PS (70 + 5/12.5/12.5 wt%) ternary blends of different blending time immediately after melt processing. The PS phase has been selectively extracted using THF. **a** Sample 7; **b** sample 8; **c** sample 9; **d** sample 10; **e** sample 11; **f** sample 12

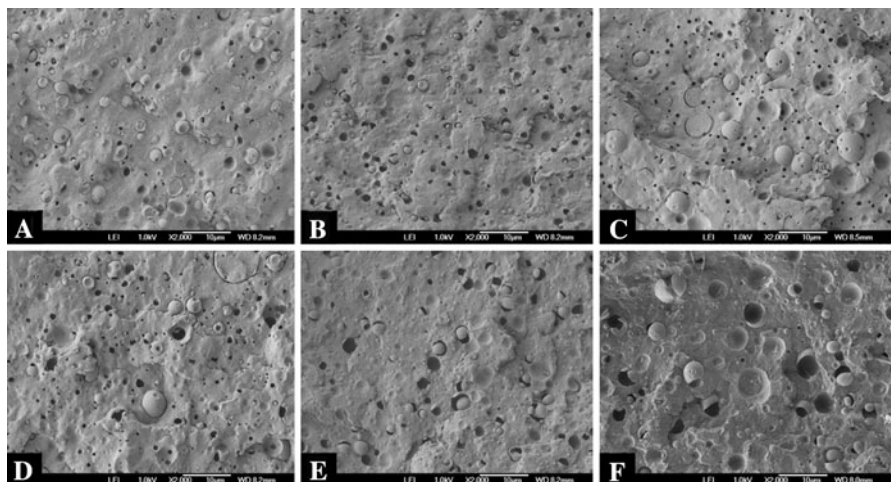


**Fig. 6** SEM micrographs of morphology of PP + PP-g-(MAH-*co*-St)/PA6/PS (70 + 5/12.5/12.5 wt%) ternary blends of different blending time immediately after melt processing. The PA6 phase has been selectively extracted using formic acid. **a** Sample 7; **b** sample 8; **c** sample 9; **d** sample 10; **e** sample 11; **f** sample 12

However, in Fig. 6, it could be seen that the encapsulation structure of the dispersed phases was greatly dependent on the charge sequence. In Fig. 6a and c, a stack formation of ternary blends with two minor phases could be observed in samples 7 and 9. While in Fig. 6b and e, when PA6 and g-PP were blended in PP matrix before the adding of PS, an encapsulation structure with PA6 as the shell and PS as the core was formed in samples 8 and 11. For samples 10 and 12, as presented in Fig. 6d and f,

the pre-mix of PS, PA6, and g-PP would be favorable for the stack forming when PP was then added.

Those phenomena are owing to the distinct interaction strength among the compatibilizer and the three components. The compatibilizer, PP-g-(MAH-*co*-St), is well miscible with the PP matrix and can react with the amine groups in PA6, and also has good affinity with the PS phase because of its styrene segments. However, the chemical bonding formed by reaction between acid anhydride groups in g-PP and the amino-groups in PA6 is much stronger than the physical affinity between PS and g-PP. Therefore, once PA6 and g-PP were charged together in PP matrix before the addition of PS, PA6-g-PP can be obtained as the compatibilizer to enhance the interface adhesion between PA6 and PP phases. Therefore, when PS was then added, the encapsulation structure of PS as the core could be formed. Besides the phase morphology mentioned above which is dominated by the charge sequence in the samples from 7 to 12, all the samples have complex phase structures.

### Mechanical properties

To investigate the influences of morphologies on the mechanical properties, samples were extruded and inject molded. The phase morphologies of the samples were as similar as the samples prepared by Haake mixer, as shown in Figs. 5 and 6.

Table 2 shows the mechanical properties of the blend samples with different charge sequences. For comparison, the mechanical properties of samples 2 and 13 prepared by single extrusion in a twin extruder were also listed. It is observed that the mechanical properties were almost unchanged for the uncompatibilized blends of samples 4–6, just as those of sample 2 prepared by single extrusion. However, for the blends with compatibilizer, great influences of charge sequence on the mechanical properties were found.

**Table 2** Mechanical properties of the multi-component polymer blends

Sample number	Tensile strength (MPa)	Flexural strength (MPa)	Break at elongation (%)	Impact strength (J/m)
Without compatibilizers				
2	25.35	32.62	3.95	9.93
4	26.10	31.89	3.36	9.17
5	25.34	33.36	3.72	9.12
6	26.36	32.56	3.19	9.87
With compatibilizers				
7	29.45	38.13	6.12	11.22
8	32.76	39.54	5.67	10.92
9	29.97	38.54	5.73	11.83
10	27.05	36.24	5.42	14.54
11	32.59	39.65	5.87	10.73
12	27.14	36.72	5.45	12.81
13	28.73	36.74	6.32	11.23

It can be seen that samples 8 and 11 with PA6 encapsulated PS phase structures showed better tensile strength and flexural strength, samples 10 and 12, in which PS, PA6, and g-PP were pre-blended in the extruder before the addition of PP matrix, demonstrated obvious improvement in impact strength.

The enhancement in tensile strength and flexural strength for samples 8 and 11 suggested that the adhesion strength between the phases was improved. It should be related to the phase structure of PS droplets encapsulated by PA6 phase existed in the PP/PS/PA6 blends of samples 8 and 11. In the presence of the compatibilizer, the bonding between PA6 phase and PP matrix is much stronger than that of PS phase and PP matrix, therefore, the interface adhesion between the PP matrix and dispersed phases in which PA6 encapsulate PS was enhanced. For samples 10 and 12, the reaction between the functional groups had already well finished before PP was charged into the blends, so there was adequate contact between PA6 and PS in the presence of g-PP. This resulted in the formation of stack structure when PP was added into the blends, which would probably be the reason that the impact strength was improved. The situation of samples 7 and 9 was similar with samples 10 and 12, but the addition of PP played a role of diluting, so the impact strength was just lower than that of samples 10 and 12. The mechanical properties of single extrusion for the compatibilized blends are just between the samples 8, 11 and samples 10, 12.

## Conclusions

In this study, the influences of component ratio of minor phases and charge sequence on the morphology and mechanical properties of PP/PS/PA6 ternary blends were studied.

For uncompatibilized blends, in spite of the component ratio and charge sequence, the core–shell morphology with PS as shell and PA6 as core in the PP matrix were unaffected. Only the thickness of the PS shell decreased with decreasing the component ratio.

While for compatibilized blends, the addition of compatibilizers resulted in a significant reduction of the dispersed droplet size, and the encapsulation structure of the dispersed phases was greatly dependent on the charge sequence.

The samples with PA6 encapsulated PS phase structures showed better tensile and flexural strength, and samples with stack structure in which PS, PA6, and g-PP were pre-blended in the extruder before the addition of PP matrix presented obvious improvement on impact strength.

**Acknowledgments** Financial supports from the National Natural Science Foundation of China (No. 20874056) and Specialized Research Fund for Doctoral Program of Higher Education (No. 200800030047) are highly appreciated.

## References

1. Guo HF, Packirisamy S, Gvozdic NV, Meier DJ (1997) Prediction and manipulation of the phase morphologies of multiphase polymer blends: I. Ternary systems. *Polymer* 38(4):785–794

2. Horiuchi S, Matchariyakul N, Yase K, Kitano T (1997) Morphology development through an interfacial reaction in ternary immiscible polymer blends. *Macromolecules* 30(12):3664–3670
3. Yoshida K, Kawamura T, Terano M, Nitta KH (2008) Effects of bulk morphology on the mechanical properties of melt-blended PP/PS blends. *J Appl Polym Sci* 109(1):211–217
4. Zhang CL, Feng LF, Gu XP, Hoppe S, Hu GH (2007) Efficiency of graft copolymers as compatibilizers for immiscible polymer blends. *Polymer* 48(20):5940–5949
5. Tang WH, Tang J, Yuan HL, Jin RG (2007) The compatibilization effect of ethylene/styrene interpolymer on polystyrene/polyethylene blends. *J Polym Sci B* 45(16):2136–2146
6. Chen JH, Zhong JC, Cai YH, Su WB, Yang YB (2007) Morphology and thermal properties in the binary blends of poly(propylene-co-ethylene) copolymer and isotactic polypropylene with polyethylene. *Polymer* 48(10):2946–2957
7. Martin P, Maquet C, Legras R, Bailly C, Leemans L, Gurn MV, Duin MV (2004) Conjugated effects of the compatibilization and the dynamic vulcanization on the phase inversion behavior in poly(butylene terephthalate)/epoxide-containing rubber reactive polymer blends. *Polymer* 45(15): 5111–5125
8. Macaubas PHP, Demarquette NR, Dealy JM (2005) Nonlinear viscoelasticity of PP/PS/SEBS blends. *Rheol Acta* 44(3):295–312
9. Souza AMC, Demarquette NR (2002) Influence of coalescence and interfacial tension on the morphology of PP/HDPE compatibilized blends. *Polymer* 43(14):3959–3967
10. Hobbs SY, Dekkers MEJ, Watkins VH (1988) Effect of interfacial forces on polymer blend morphologies. *Polymer* 29(9):1598–1602
11. Reigner J, Favis BD (2000) Control of the subinclusion microstructure in HDPE/PS/PMMA ternary blends. *Macromolecules* 33(19):6998–7008
12. Guo HF, Packirisamy S, Gvozdic NV, Meier DJ (1997) Prediction and manipulation of the phase morphologies of multiphase polymer blends: II. Quaternary systems. *Polymer* 38(19):4915–4923
13. Palmer G, Demarquette NR (2003) New procedure to increase the accuracy of interfacial tension measurements obtained by breaking thread method. *Polymer* 44(10):3045–3052
14. Morita AT, Carastan DJ, Demarquette NR (2002) Influence of drop volume on surface tension evaluated using the pendant drop method. *Colloid Polym Sci* 280(9):857–864
15. Demarquette NR, Kamal MR (1994) Interfacial tension in polymer melts. I: an improved pendant drop apparatus. *Polym Eng Sci* 34(24):1823–1833
16. Kamal MR, Fook RL, Demarquette NR (1994) Interfacial tension in polymer melts. Part II: effects of temperature and molecular weight on interfacial tension. *Polym Eng Sci* 34(24):1834–1839
17. Demarquette NR, Kamal MR (1998) Influence of maleation of polypropylene on the interfacial properties between polypropylene and ethylene-vinyl alcohol copolymer. *J Appl Polym Sci* 70(1):75–87
18. Chaffin KA, Knutsen JS, Brant P, Bates FS (2000) High-strength welds in metallocene polypropylene/polyethylene laminates. *Science* 288:2187–2190
19. Chaffin KA, Bates FS, Bryant P, Brown GM (2000) Semicrystalline blends of polyethylene and isotactic polypropylene: improving mechanical performance by enhancing the interfacial structure. *J Polym Sci B* 38(1):108–121
20. Valera TS, Morita AT, Demarquette NR (2006) Study of morphologies of PMMA/PP/PS ternary blends. *Macromolecules* 39(7):2663–2675
21. Reigner J, Favis BD, Heuzey MC (2003) Factors influencing encapsulation behavior in composite droplet-type polymer blends. *Polymer* 44(1):49–59
22. Graebling D, Muller R, Palierne JF (1993) Linear viscoelastic behavior of some incompatible polymer blends in the melt. Interpretation of data with a model of emulsion of viscoelastic liquids. *Macromolecules* 26(2):320–329
23. Kim BK, Kim MS (1993) Viscosity effect in polyolefin ternary blends and composites. *J Appl Polym Sci* 48(7):1271–1278
24. Omonov TS, Harrats C, Groeninx G (2005) Co-continuous and encapsulated three phase morphologies in uncompatibilized and reactively compatibilized polyamide 6/polypropylene/polystyrene ternary blends using two reactive precursors. *Polymer* 46(26):12322–12336
25. Omonov TS, Harrats C, Groeninx G, Moldenaers P (2007) Anisotropy and instability of the co-continuous phase morphology in uncompatibilized and reactively compatibilized polypropylene/polystyrene blends. *Polymer* 48(18):5289–5303
26. Russo AP, Nauman EB (2000) Modeling the effect of compatibilizers in the coarsening of ternary polymer blends with core-shell morphology. *J Polym Sci B* 38(10):1301–1306

27. Freitas CA, Valera TS, Souza AMC, Demarquette NR (2007) Morphology of compatibilized ternary blends. *Macromol Symp* 247(1):260–270
28. Zhang XM, Kim JK (1998) Interfacial tension measurement with the Neumann triangle method. *Macromol Rapid Commun* 19(9):499–504
29. Virgilio N, Aurèle CM, Favis BD (2009) Novel self-assembling close-packed droplet array at the interface in ternary polymer blends. *Macromolecules* 42(9):3405–3416
30. Lusinov I, Pagnouille C, Jérôme R (2000) Ternary polymer blend with core–shell dispersed phases: effect of the core-forming polymer on phase morphology and mechanical properties. *Polymer* 41(19):7099–7109
31. Hyun DC, Jeong U, Ryu DY (2007) A simple approach to determine the equilibrium shape and position of sandwiched polymer droplets. *J Polym Sci B* 45(19):2729–2738
32. Wang D, Xie XM (2006) Novel strategy for ternary polymer blend compatibilization. *Polymer* 47(23):7859–7863
33. Li Y, Xie XM, Guo BH (2001) Study on styrene-assisted melt free-radical grafting of maleic anhydride onto polypropylene. *Polymer* 42(8):3419–3425
34. Xie XM, Chen NH, Guo BH, Li S (2000) Study of multi-monomer melt-grafting onto polypropylene in an extruder. *Polym Int* 49(12):1677–1683
35. Jannerfeldt G, Boogh L, Mañson JAE (1999) Influence of hyperbranched polymers on the interfacial tension of polypropylene/polyamide-6 blends. *J Polym Sci B* 37(16):2069–2077